# Rheological Properties and Molecular Structure of Tunicate Cellulose in LiCl/1,3-Dimethyl-2-imidazolidinone

Nobutake Tamai, Daisuke Tatsumi, and Takayoshi Matsumoto*

*Division of Forest and Biomaterials Science, Graduate School of Agriculture, Kyoto University, Kyoto 606-8502, Japan*

*Received July 11, 2003; Revised Manuscript Received November 4, 2003*

Solution properties and molecular structure of tunicate cellulose (TC), an animal cellulose from *Halocynthia roretzi*, were investigated in terms of rheological and dilute solution properties. The solvent used is 8 wt % LiCl/1,3-dimethyl-2-imidazolidinone (DMI). A solution of dissolving pulp (DP), derived from plant, was also used for comparison. The weight-average molecular weight, $M_w$, and the limiting viscosity number, $[\eta]$, of the TC were evaluated to be $413 \times 10^6$ and 2645 mL/g, respectively. The TC solution showed the same concentration dependence of $G_N$ ($G_N = 5.49 \times 10^6 \phi_w^{2.1_4}$ Pa; $\phi_w$: weight fraction of cellulose in solution; $G_N$: plateau modulus) as the DP solution and, moreover, also as the solution of cotton linter (CC) in 8 wt % LiCl/*N*,*N*-dimethylacetamide (DMAc). This exponent of $2.1_4$ indicates that network structure by entanglements was formed in these solutions. According to the theory of Fetters et al., moreover, such identity means that all of these celluloses have the identical chain structure though their biological origins are far different. On the other hand, the $\phi_w$-dependence of $\eta_0 - \eta_s$ ($\eta_0$ = zero shear rate viscosity of solution; $\eta_s$ = solvent viscosity) was different between the TC and the DP solution in the semidilute regime: the TC solution exhibited $\eta_0 - \eta_s \propto \phi_w^{7.5}$ and the DP solution $\eta_0 - \eta_s \propto \phi_w^4$. According to the theory of Doi−Edwards, this exponent of 4 (the DP solution) indicates that the DP behaves as flexible polymers in the solution. In contrast, the dependence for the TC solution seems unexplainable on the basis of molecular theories. This difference probably signifies the difference in the relaxation process or mechanism in entanglement systems.

## Introduction

Tunicin, or tunicate cellulose, is a cellulose from ascidians,[1,2] a kind of sea animal. It is well-known that a wide variety of living things, including ascidians, produce cellulose, and recent biological and genetic studies on them have given us more information on their biological features such as biosynthesis pathways and synthases.[3−5] As for the physicochemical properties of native celluloses, however, few comparative investigations have been made in terms of the their biological origins.

One quite interesting finding is that the crystalline form of native cellulose is composed of two crystalline allomorphs, $I_\alpha$ and $I_\beta$, and that the different celluloses in their origins have different mixing ratios of $I_\alpha$ and $I_\beta$.[6,7] Bacterial and algal celluloses have an $I_\alpha$-rich crystalline form, whereas $I_\beta$ is dominant in the celluloses from higher plants including cotton and ramie. In addition, tunicate cellulose has an almost pure crystalline form of $I_\beta$ (more than 99% $I_\beta$).[8] Atalla has recently reported on the species specificity of the structures of native celluloses in terms of quantification of their diversity of morphology on wide scales from the order of the crystalline structure to that of the fibril length.[9] Unfortunately, most of these studies have focused mainly on solid structures of cellulose; that is, their properties reflect states of aggregation of cellulose molecular chains. Thus, molecular properties of a whole structure of a single chain have scarcely been discussed. This is probably due to the prevalent belief that all celluloses are identical in the molecular properties irrespective of their origins and different biosynthetic pathways. However, it is considerably important to verify this general belief because it may be blindly accepted without full scientific confirmation.

The scarce elucidation of molecular properties and structures of a single chain of celluloses is also due to the practical difficulty, that is, the lack of convenient solvents for cellulose, because the elucidation requires dissolution of cellulose in general. A great number of solvents have been discovered for cellulose, but many of these have some disadvantages such as toxicity and low stability. Around 1980, it was discovered that *N*,*N*-dimethylacetamide (DMAc) containing lithium chloride (ca. 8−9 wt %) can dissolve cellulose.[10,11] This solvent has advantages in many respects over traditional ones at least for experimental use; that is, it is a good solvent, is colorless, and has lower toxicity, and moreover, the resulting solution is quite stable. McCormick et al. have already made many fundamental studies including the preparation of a number of derivatives[12] and dilute solution properties,[13] but many other solution properties of cellulose in LiCl/DMAc, especially rheological properties in semidilute and concentrated regions, still remain hardly revealed. Recent extensive and rigorous studies on cellulose

* To whom correspondence may be addressed. Phone: +81-75-753-6246. Fax: +81-75-753-6300. E-mail: matsutk@kais.kyoto-u.ac.jp.

10.1021/bm034236h CCC: $27.50 
Published on Web 01/14/2004

solutions with other solvents (e.g., Cd-tren) by Saalwächter and Burchard[14,15] have revealed dynamic and static molecular properties of cellulose in dilute and semidilute solutions based on familiar theories of polymer physics. As far as we know, however, no one has discussed differences in solution properties of celluloses from various biological sources.

In the previous papers,[16,17] we have reported that some differences were observed in the solubility to 8 wt % LiCl/DMAc for celluloses from plants, bacteria, and ascidians. Moreover, we demonstrated the differences in rheological properties between plant and bacterial celluloses and explained them on the basis of the difference in molecular structure of higher order. Unfortunately, however, we were not able to investigate the solution properties of tunicate cellulose because it did not dissolve in 8 wt % LiCl/DMAc. At the beginning of the utilization of LiCl/DMAc, only LiCl/*N*-methyl-2-pyrrolidinone (NMP) was known as another cellulose solvent containing LiCl.[18] A few years later, 1,3-dimethyl-2-imidazolidinone (DMI) was found to be a substitute for DMAc and NMP.[19,20] We have recently found that this solvent of 8 wt % LiCl/DMI can dissolve tunicate cellulose.[16] In the present study, we discuss the molecular structure and rheological properties of tunicate cellulose (TC) in 8 wt % LiCl/DMI solution in comparison with those of dissolving pulp (DP) in the same solvent and also with those of cotton linter cellulose (CC) in 8 wt % LiCl/DMAc from previous work.[17]

## Materials and Methods

**Materials and Preparation of Solutions.** The cellulose sample of tunicate cellulose (TC) is derived from *Halocynthia roretzi*. Softwood dissolving pulp (DP) was also used, which was manufactured by Nippon Paper Industries Co., Ltd. All samples were not unfractionated, and no information about the polydispersity of the molecular weight is available.

As to how to dissolve the cellulose samples in 8 wt % LiCl/DMI, we referred to the method of the dissolution in 8 wt % LiCl/DMAc reported by McCormick et al.[13] The dissolution method involves the following solvent-exchange procedure. First, each cellulose sample was suspended in distilled water for 24 h at room temperature. After filtration, it was immersed into acetone for 48 h and subsequently into *N*,*N*-dimethylacetamide (DMAc) for 24 h at room temperature. The sample was vacuum-dried for ca. 48 h at 60 °C after the solvent-exchange procedure. The dried sample was dissolved in 8 wt % LiCl/1,3-dimethyl-2-imidazolidinone (DMI) at room temperature. A homogeneous solution was obtained in 6−9 months for the TC depending on the concentration of the solution.

**Static Light-Scattering Measurements.** A light-scattering photometer of SLS-5000HM (Otsuka Electronics Co., Ltd., Osaka) was used for static light-scattering (SLS) measurements. The photometer has a He−Ne laser source with a wavelength of 633 nm. The sample solutions were filtered by membrane filters first with a pore size of 0.45 $\mu$m and then with a pore size of 0.2 $\mu$m several times before measurements. We used the value of 0.0406 mL/g as specific refractive index increment, d*n*/d*c*, for static light-scattering measurements.[21]

The reciprocal reduced scattered intensity, $Kc/R_\theta$, at the scattering angle $\theta$ can be generally expressed in terms of a virial expansion as a power series in $c$ ($c$: polymer concentration in g/mL). In many cases, SLS measurements are performed for a dilute solution, and then the virial expansion can be truncated after the second-order term:

$$\frac{Kc}{R_\theta} = \frac{1}{M_w}\left[1 + \frac{1}{3}\langle R_g^2\rangle_z q^2\right] + 2A_2 c \qquad \left(q = \frac{4\pi}{\lambda_0/n}\sin\frac{\theta}{2}\right) \quad (1)$$

where $K$, $R_\theta$, $M_w$, $\langle R_g^2\rangle_z$, $\lambda_0$, $n$, and $A_2$ denote an optical constant, the excess Rayleigh ratio of the solution at $\theta$, the weight-average molecular weight, the $z$-average mean square radius of gyration, the wavelength of the incident beam, the refractive index of the solvent, and the second viral coefficient, respectively. The value of $q$ corresponds to the magnitude of the scattering vector, **q**. According to eq 1, the determination of $M_w$ involves double linear extrapolations of $Kc/R_\theta$ as a function of $c$ and $q^2$ to $c = 0$ and $q^2 = 0$. A Zimm diagram, a plot of $Kc/R_\theta$ versus $q^2 + Pc$, allows simultaneously this double extrapolation, where $P$ is an arbitrary constant. Moreover, it also provides the values of $A_2$ and $\langle R_g^2\rangle_z^{1/2}$. Owing to the facility, thus, the Zimm diagram is usually used for the determination of these molecular parameters. For a polymer solution containing huge macromolecules, however, their determination should be more careful; that is, each linear extrapolation to $c = 0$ and $q^2 = 0$ had better be separately carried out to verify the validity of the linear approximation. Especially regarding the linear extrapolation to $c = 0$ (i.e., the determination of $M_w$ and $A_2$), a Debye plot, which shows the concentration dependence of $(Kc/R_\theta)_{\theta\to 0}$, is useful and preferable because it allows one to ascertain clearly the dilute region and then provides the more accurate values of $M_w$ and $A_2$. A Berry plot, which shows the relationship between the square root of $(Kc/R_\theta)_{\theta\to 0}$ and $c$, is also quite useful for their careful determination. This plot will provide the linear relationship in a wider $c$ region than the Debye plot. Thus, we analyzed the SLS data using these three types of plots for the molecular characterization of the TC.

**Measurements for Viscoelastic Properties and Limiting Viscosity Number.** A cone-plate-type rheometer, Rheosol-G2000 (UBM Co., Ltd., Kyoto), was used for dynamic viscoelasticity and steady-flow measurements. Radii of the cone and plate were 50 mm, and the angle of the cone was 2°. A reservoir was equipped for the rheometer to prevent the sample from drying during measurements. The dynamic viscoelasticity measurements were performed at various temperatures ranging from −15 to 110 °C. The range of the oscillatory frequency is from $10^{-2}$ to $10^2$ Hz at each temperature. All of the data were reduced to the data at a reference temperature of 30 °C by the time−temperature superposition principle.[22] The steady flow measurements were carried out at 30 °C within the shear rate range from $3.0 \times 10^{-3}$ to $10^2$ s$^{-1}$. For the TC solution of $\phi_w = 0.007$ ($\phi_w$: the weight fraction of polymer), the measurements were done at the temperature from 30 to 90 °C and all of the data were reduced to the data at 30 °C.

The plateau modulus, $G_N$, was evaluated using a generalized Maxwell model.[17] We first determined how to choose

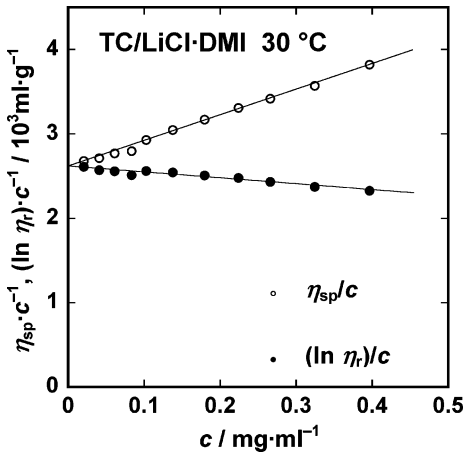


**Figure 1.** Concentration dependence of $\eta_{sp}/c$ (○) and (ln $\eta_r$)/$c$ (●) for TC solutions in 8 wt % LiCl/DMI at 30 °C. Intercept of each line at $c = 0$ corresponds to [$\eta$].

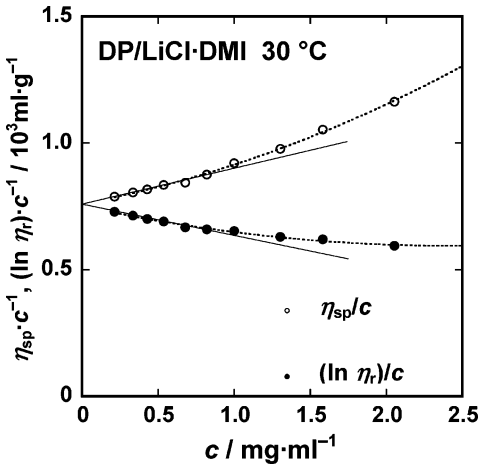


**Figure 2.** Concentration dependence of $\eta_{sp}/c$ (○) and (ln $\eta_r$)/$c$ (●) for DP solutions in 8 wt % LiCl/DMI at 30 °C. Intercept of each line at $c = 0$ corresponds to [$\eta$].

the relaxation times; that is,

$$\tau_p = x^{p-1}\tau_1 \qquad (0 < x < 1, p = 1, 2, ..., n) \qquad (5)$$

where $\tau_p$, $\tau_1$, and $x$ denote the relaxation time, the longest relaxation time, and a constant independent of $p$, respectively. Based on these relaxation times, the relaxation spectra were calculated by determining the values of $\tau_1$, $n$, and all of the relaxation intensity, $G_p$, of $p$th relaxation mode in the model for all of the TC and the DP solutions that exhibited the viscoelastic behavior of an entangled polymer system. Though this method cannot achieve the unique determination of the relaxation spectra, the incompletion of the unique determination hardly affects the $G_N$ value because any spectrum that can reproduce the original viscoelastic curves is expected to provide similar $G_N$ values. Thus, the accurate estimation of $G_N$ requires experimental data of $G'(\omega)$ and $G''(\omega)$ over wide range of $\omega$ where the plateau region is clearly observed. Further, we tried to reduce the effect of artifacts from the incompletion on the estimation of the $G_N$ value by applying the similarity in the shape of viscoelastic curves observed for the same kind of solutions at different concentrations.

Limiting viscosity number was determined with an Ubbelohde-type capillary viscometer. All measurements were made in a constant-temperature bath regulated at 30 °C.

## Results

**Molecular Characterization of Tunicate Cellulose.** The capillary viscometric measurement provides the relative viscosity, $\eta_r$ (=$\eta_0/\eta_s$; $\eta_0$: zero shear rate viscosity of solution; $\eta_s$: solvent viscosity), or the specific viscosity, $\eta_{sp}$(=$\eta_r$ − 1), of the polymer solution. Both plots of $\eta_{sp}/c$ and (ln $\eta_r$)/$c$ versus $c$ give two straight lines with an identical intercept at $c = 0$; the intercept corresponds to the limiting viscosity number, [$\eta$]. The Huggins constant, $k_H$, can also be estimated independently from the slopes of both straight lines.[23] The $c$-dependence of $\eta_{sp}/c$ and (ln $\eta_r$)/$c$ is shown in Figures 1 and 2 for the TC and the DP solutions in 8 wt % LiCl/DMI, respectively. For each cellulose solution, the extrapolated intercepts at $c = 0$ of both plots agreed within the experimental error. This agreement shows the accuracy of the measurements. The values of [$\eta$] and $k_H$ are listed in Table 1 for both cellulose solutions.

**Table 1.** Molecular Characteristics of TC and DP in 8 wt % LiCl/DMI Solution and of CC, DP, and BC in 8 wt % LiCl/DMAc Solution

| sample | solvent | $10^{-4}M_w$ | $\langle R_g^2\rangle_z^{1/2}$, nm | $10^3A_2$, g$^{-2}$·ml·mol | [$\eta$], mL·g$^{-1}$ | $K'$ |
|---|---|---|---|---|---|---|
| TC | LiCl/DMI | 413 | 114 | 0.923 | 2645 | 0.42 |
| DP | LiCl/DMI | | | | 756 | 0.25 |
| CC[a] | LiCl/DMAc | 170 | 109 | 1.33 | 1504 | 0.43 |
| DP[a] | LiCl/DMAc | 98.2 | | 2.16 | 704 | 0.42 |
| BC[a] | LiCl/DMAc | 192 | 98.1 | 1.12 | 935 | 0.31 |

[a] The data of this sample are from our previous paper.[17]

The results from the SLS measurements are shown in Figure 3a in the form of a Debye plot for the TC solution at 25 °C. The linear relation was observed between $(Kc/R_\theta)_{\theta\to 0}$ and $c$ in the region of $c$ less than ca. 0.2 mg/mL. By the method of the linear extrapolation to $c = 0$ with the data of $(Kc/R_\theta)_{\theta\to 0}$ in this $c$-region, thus, the values of $M_w$ and $A_2$ were estimated to be $4.13 \times 10^6$ and $0.923 \times 10^{-3}$ g$^{-2}$·mL·mol, respectively. These values are listed in Table 1. Above the concentration of 0.2 mg/mL, the linear approximation broke down and the deviation of $(Kc/R_\theta)_{\theta\to 0}$ from the straight line became gradually larger with increasing concentration. This means that the second-order term in the expression of $Kc/R_\theta$ as a virial expansion in powers of $c$ cannot be regarded as a trivial term; that is, the TC solution above that concentration is not a dilute solution for the scattering measurement in a strict sense. That concentration corresponds to the overlap concentration, $c^*$, at which the polymer molecules start to overlap each other, and the value of $c^*$ can be determined more definitely as $1/(M_wA_2)$ (= 0.262 mg/mL). In the case of lower $c^*$ systems, it is quite useful for accuracy to apply also a Berry plot. This plot permits a linear approximation in the wider $c$-region than the Debye plot. Figure 3a also shows the results from the SLS measurements as a Berry plot. Actually, a linear relation was observed between them in the whole $c$-region where the measurements were carried out. The values of $M_w$ and $A_2$ evaluated from the Berry plot were in good agreement

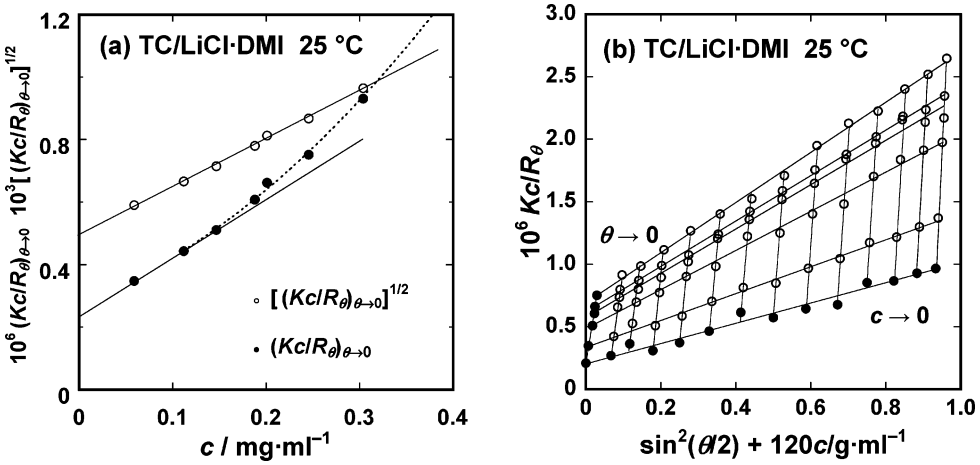


**Figure 3.** Debye plot, $(Kc/R_\theta)_{\theta\to0}$ vs $c$, and Berry plot, $[(Kc/R_\theta)_{\theta\to0}]^{1/2}$ vs $c$ (a) and (b) Zimm plot, $Kc/R_\theta$ vs $\sin^2(\theta/2) + Pc$, for TC solution in 8 wt % LiCl/DMI at 25 °C. $K$, $c$, $R_\theta$, and $P$ represent optical constant, concentration, excess Rayleigh ratio at scattering angle $\theta$, and a constant (here, $P = 120$).

with those from the Debye plot within the experimental error: $M_w = 4.07 \times 10^6$; $A_2 = 0.905 \times 10^{-3}$ g$^{-2}$·mL·mol.

Figure 3b shows a Zimm plot for the TC solution at 25 °C with $P = 120$ to estimate the value of $\langle R_g^2\rangle_z^{1/2}$. Both of the extrapolated data, $(Kc/R_\theta)_{c\to0}$ and $(Kc/R_\theta)_{\theta\to0}$, are represented by filled symbols. As is clear from the figure, the $q^2$-dependence of $(Kc/R_\theta)_{c\to0}$ appears to exhibit almost linear relation, and thus, the value of $\langle R_g^2\rangle_z^{1/2}$ was estimated to be 114 nm for the TC from the slope of the straight line representing the dependence. Here, we must note that this $R_g$ value is derived from the measurements out of a proper $q$-range, because the $R_g$ value should be normally determined in the $q$-range where the relation of $\langle R_g^2\rangle_z q^2 < 1$ holds. Out of the ideal $q$-range, the dependence will no longer exhibit the linear relation in general, and it can be expressed as a complicated function of $q$ depending on the shape of a solute polymer. For the TC solutions, the apparent linear relation may be due to the polydispersity of the sample. The accuracy of the $R_g$ value, therefore, is not high. Actually, the $R_g$ value of the TC seems considerably small for the large molecular weight in comparison with that of the CC in 8 wt % LiCl/DMAc solution. These points are discussed later in the section "Size of the TC Molecule".

**Rheological Measurements.** The dependence of storage modulus, $G'$, and loss modulus, $G''$, on the reduced angular frequency, $\omega a_T$, is shown in Figure 4 for the TC solution in 8 wt % LiCl/DMI at various weight fractions of polymer, $\phi_w$, ranging from 0.002 to 0.01. All of these curves are shifted upward in the figure by a factor $B$ except for the curves at $\phi_w = 0.002$. The solid lines in the figure show the calculation curves using a generalized Maxwell model with an appropriate combination of $n$ relaxation times, $\tau_p$ ($p = 1, 2, ..., n$). Details are described in our previous paper.[17]

At $\phi_w = 0.002$, the curve of $G''$ was larger than that of $G'$ in the whole $\omega$-region where the measurements were carried out; that is, the plateau region was not observed even in the sufficiently higher frequency region. Such behavior is observed for dilute solutions, of which dynamic viscoelastic behavior is similar to that of Rouse model.[24,25] Accordingly, these curves of $G'$ and $G''$ signify that the development of the network structure by entanglements is immature in the

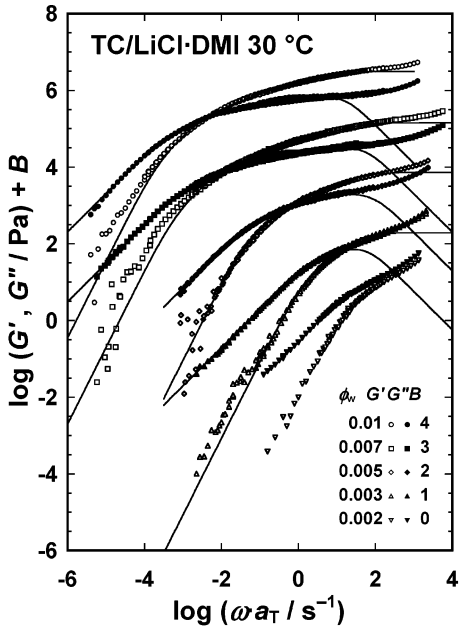


**Figure 4.** Dependence of dynamic storage modulus, $G'$ (open symbols), and loss modulus, $G''$ (filled symbols), on reduced angular frequency, $\omega a_T$, for TC solutions at various weight fraction of polymer, $\phi_w$, ranging from 0.002 to 0.01. Reference temperature is 30 °C. These curves are shifted vertically by a factor $B$ except for those at $\phi_w = 0.002$. Solid lines represent the curves reproduced by calculation using a generalized Maxwell model.[17]

solution at $\phi_w = 0.002$. At $\phi_w = 0.003$, the plateau region began to appear at higher frequencies. As $\phi_w$ increased further, the plateau region became longer and the flow region, where the relations of $G' \propto \omega^2$ and $G'' \propto \omega^1$ hold, accordingly shifted toward lower frequencies. Such transitional change in the viscoelastic behavior with increasing concentration is typical of many flexible polymer solutions.

Figure 5 shows the similar plot for the DP solutions in 8 wt % LiCl/DMI at different weight factions of the DP ranging from 0.007 to 0.05 and at the reference temperature of 30 °C. The DP solution at $\phi_w = 0.007$ showed the Rouse-like behavior, signifying that the solution was not concentrated enough to form entanglements of polymer chains. As the concentration increased, the plateau region appeared at higher frequencies. This indicates the formation of the entangle-

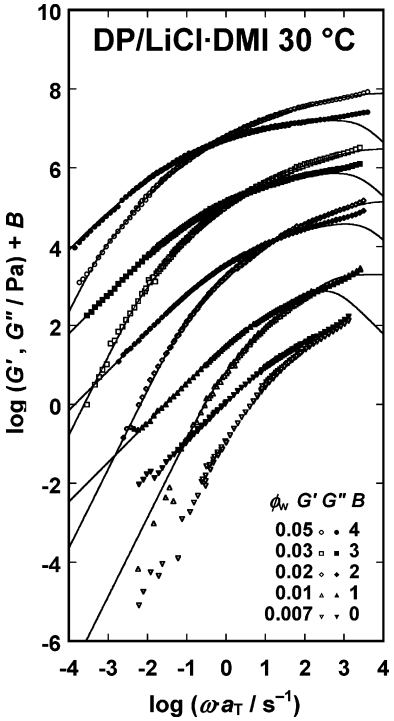


**Figure 5.** Dependence of dynamic storage modulus, $G'$ (open symbols), and loss modulus, $G''$ (filled symbols), on reduced angular frequency, $\omega a_T$, for DP solutions at various weight fraction of polymer, $\phi_w$, ranging from 0.007 to 0.05. Reference temperature is 30 °C. The curves are shifted vertically by a factor $B$ except for those at $\phi_w = 0.007$. Solid lines represents the curves reproduced by calculation using a generalized Maxwell model.[17]

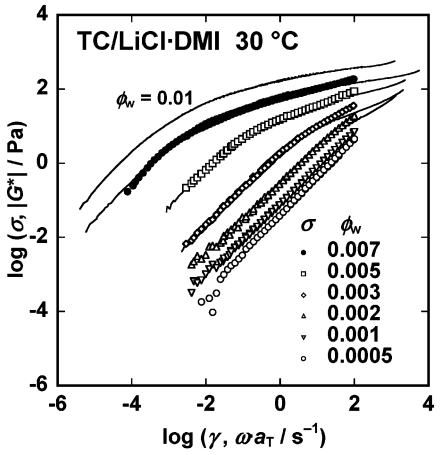


**Figure 6.** Dependence of shear stress, $\sigma$ (plots), on shear rate, $\dot{\gamma}$, at 30 °C for TC solutions at various weight fraction of polymer, $\phi_w$, ranging from 0.0005 to 0.07. Solid lines represent dependence of complex modulus, $G^*$, on reduced angular frequency, $\omega a_T$, at 30 °C.

ments. These rheological behaviors are similar to the TC solutions and also typical of flexible polymer solutions.

Figure 6 shows the dependence of the stress, $\sigma$, on the shear rate, $\dot{\gamma}$, at 30 °C for the TC solutions at different weight fractions of the TC ranging from 0.0005 to 0.007 in the form of a double logarithmic plot. The TC solutions at lower $\phi_w$ showed Newtonian flow in almost all of the $\dot{\gamma}$-region where the measurements were performed. As $\phi_w$ increased, non-Newtonian flow was observed in the higher $\dot{\gamma}$-region. This flow behavior is commonly observed for polymer solutions. Figure 6 shows also the dependence of the absolute value of a complex modulus, $|G^*|$, defined as $|G^*| = \sqrt{G'^2+G''^2}$, on the reduced angular frequency with solid lines. The empirical Cox−Merz rule states that the value of $|G^*|$ at an arbitrary angular frequency must be equal to that of $\sigma$ at the shear rate of the identical value.[26] Actually, many polymeric systems show the validity of the rule. The TC solutions also showed good agreement between $|G^*|$ and $\sigma$, although slight disagreement was observed partially in the higher $\dot{\gamma}$- and $\omega$-region.

## Discussion

**Dispersion State in LiCl/DMI and LiCl/DMAc Systems.** Table 1 gives the characteristic values of $M_w$, $A_2$, $\langle R_g^2\rangle_z^{1/2}$, $[\eta]$, and $k_H$ for the TC and the DP solutions in 8 wt % LiCl/DMI. For comparison, it also gives the characteristic data of the solutions of the DP, cotton linter (CC), and bacterial cellulose (BC) in 8 wt % LiCl/DMAc from our previous work.[17] The value of $[\eta]$ of the DP molecule in 8 wt % LiCl/DMI is 1.07 times larger than that in 8 wt % LiCl/DMAc. This difference in the $[\eta]$ value indicates that the DP molecule can take more extended conformation in the LiCl/DMI system than in the LiCl/DMAc system. To be sure, the solvent power of LiCl/DMI seems greater than that of LiCl/DMAc, considering that 8 wt % LiCl/DMI can dissolve tunicate cellulose while 8 wt % LiCl/DMAc does not. In terms of the $R_g$ value, however, the difference can be regarded as negligible because $[\eta]$ is proportional to $R_g^3M^{-1}$ for a flexible polymer. Thus, the difference reflects the negligible degree of spatial expansion of a single molecular chain of the DP in solution. This means that the difference of the conformation of the DP in both solvents is insignificant. This point is discussed later again from the viewpoint of the rheological properties of the solutions.

The value of $k_H$ of the TC/LiCl/DMI solution is similar to those of the DP/LiCl/DMAc and the CC/LiCl/DMAc solutions, whereas those of the DP/LiCl/DMI and BC/LiCl/DMAc solutions are somewhat smaller. The quantitative analysis and discussion on this difference seem insignificant for their intricacy, because the thermodynamic meaning of its absolute value is rather ambiguous. It is empirically known that its value is around 0.3 for good solvent systems and 0.5−1.0 for Θ systems almost independent of the molecular weight and the sort of polymers and solvents except for polyelectrolyte aqueous systems.[27] Moreover, it is also known that its value is sensitive to chain aggregation and that the association among polymers tends to make its value higher (over 1).[27] According to these generalizations, it is qualitatively expected that TC molecules are dispersed molecularly in the dilute solution without forming some complex association as are the other kinds of cellulose samples.

**Size of the TC Molecule.** Comparing with the molecular structure of the CC in 8 wt % LiCl/DMAc will lead to useful speculation on the structure of the TC molecule, because the structural properties of the CC have been elucidated in the previous paper[17] by comparing with existing data from extensive studies by McCormick et al.[13] and Saalwächter et al.[14,15] As a result, for example, the exponent $\upsilon_\eta$ in the Mark−Houwink−Sakurada equation of $[\eta] \propto M^{\upsilon_\eta}$ has been estimated to be 0.85 from the concentration dependence of zero

shear rate viscosity of the solution in the semidilute region for the plant cellulose solution in 8 wt % LiCl/DMAc. We must note here again that McCormick et al.[13] had already determined the value of $\upsilon_\eta$ to be 1.19 in a general way for dilute solutions, although we have already discussed the difference in the previous paper.[17]

From the value of $\upsilon_\eta$, the exponent $\upsilon$ ($R_g \propto M^\upsilon$) can be calculated to be $0.61_7$ using the equation of $\upsilon_\eta = 3\upsilon - 1$ for flexible polymers.[28] Assuming that the TC molecule has the same structure as the CC molecules in 8 wt % LiCl/DMAc solution with the identical value of the exponent $\upsilon$ of $0.61_7$, the $R_g$ value of the TC molecule is expected to be 188 nm. This is much larger than $\langle R_g^2\rangle_z^{1/2}$ of 114 nm determined by the SLS measurements.

To examine the reliability of the $R_g$ value of the TC from the SLS measurements, we tried to estimate it in another way. Based on the mean field theory, $c^*$ can be roughly related to $R_g$ by the following simple equation[29] on the assumption of the conservation of the volume occupied with a single dispersed particle in the solution:

$$c^* \approx \frac{M}{N_A \frac{4}{3}\pi R_g^3} \tag{2}$$

where $N_A$ represents Avogadro's constant. As mentioned previously, $c^*$ is determined as $1/(A_2M_w)$. We confirmed that the $R_g$ value from this method is in fairly good agreement with the value of $\langle R_g^2\rangle_z^{1/2}$ from SLS measurements within the relative difference of $\pm 10-15\%$ using some existing data including cellulose solutions.[14,30,31] For the TC solution, $R_g$ is calculated to be 184 nm from the $c^*$ of 0.262 mg/mL. This is much larger than $\langle R_g^2\rangle_z^{1/2}$ of 114 nm, but interestingly, very close to the expectation of 188 nm, which has been calculated above on the assumption that the TC molecule has the same structure as the CC molecule. This result suggests the possibility that the TC and the CC molecules have the same chain structure. This suggestion will be strongly supported by the results of the concentration dependence of the plateau modulus of the solution, which are discussed later.

**Angular Frequency Dependence of Dynamic Moduli.** As shown in Figures 4 and 5, the TC and the DP solutions showed typical viscoelastic behavior of many flexible polymer solutions. Compared to the DP solutions, the TC solutions showed such transitional change with increasing concentration within a much narrower concentration range. Moreover, the plateau region was clearly observed at much lower concentration. These are probably because the TC molecules are much larger than the DP molecules. The DP solutions showed viscoelastic curves with considerably longer transition regions from the plateau to the terminal zone. Such a feature is often observed for polymeric systems having relatively wider molecular weight distribution. Therefore, the DP is expected to have a large degree of polydispersity. This speculation may be reasonable because the DP is a cellulose sample that was isolated from wood by a number of severe chemical treatments.

**Apparent Activation Energy for Viscoelastic Relaxation.** Dependence of viscoelastic behavior on temperature provides some useful information on the qualitative speculation of the relaxation process of polymer chains. As shown already in Figures 4 and 5, the time−temperature superposition principle can be applied to the viscoelastic curves of the TC and the DP solutions in 8 wt % LiCl/DMI according to the method of reduced variables.[22] This suggests that the relaxation mechanism does not change with varying temperature within the temperature range from −15 to 110 °C.

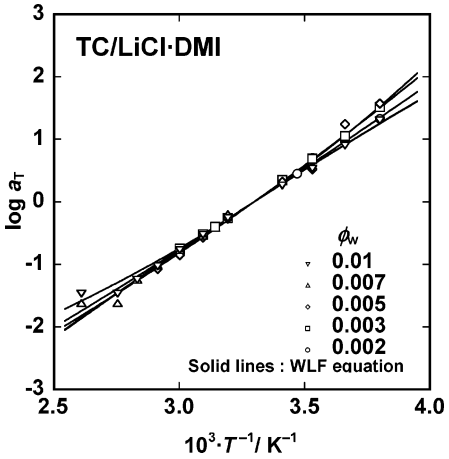


**Figure 7.** Relationship between log $a_T$ and $1/T$ for TC solutions at various weight fraction of polymer, $\phi_w$, ranging from 0.002 to 0.01, where $a_T$ and $T$ represent shift factor and absolute temperature, respectively. Solid lines show results of curve fitting using WLF equation. Apparent activation energy for viscoelastic relaxation, $\Delta E_a$, can be evaluated with constants $c_1$ and $c_2$ in the WLF equation (see also text).

The apparent activation energy for viscoelastic relaxation, $\Delta E_a$, can be evaluated from the temperature dependence of the shift factor, $a_T$. Figure 7 shows the relationship between the natural logarithm of $a_T$ and the reciprocal of the absolute temperature, $1/T$, for the TC solution. In the higher temperature region (i.e., smaller $1/T$ region), the linear relationship between $\ln a_T$ and $1/T$ was observed, which can be expressed by an Arrhenius-type equation. As the temperature approached the freezing point of the solvent (ca. −20 °C: $1/T \approx 3.95 \times 10^{-3}$ K$^{-1}$), however, the quantities of ($\ln a_T$) steeply increased with increasing $1/T$, which indicates that the Arrhenius-type equation fails to express the relation. Similar behavior is generally observed for many synthetic polymer solutions and melts around the glass transition point. In such a case, $\Delta E_a$ should be estimated using the WLF equation,[22] which can well represent the deviation from the linear relationship near the glass transition temperature:

$$\ln a_T = \frac{-c_1(T - T_s)}{c_2 + (T - T_s)} \tag{3}$$

where $c_1$ and $c_2$ denote experimental constants and $T_s$ is a reference temperature (here, $T_s = 303$ K). As shown in Figure 7 as solid lines, the WLF equation can well represent the experimental results of ($\ln a_T$) for the TC solution with appropriate values for the constants of $c_1$ and $c_2$, which are listed in Table 2. Then, $\Delta E_a$ at the reference temperature was estimated from the following equation:

$$\Delta E_a(T{=}T_s) = R\frac{\mathrm{d}\ln a_T}{\mathrm{d}(1/T)}\Big|_{T=T_s} = R(c_1/c_2)T_s^2 \tag{4}$$

**Table 2.** Constants $c_1$ and $c_2$ in WLF Equation for TC Solution

| $\phi_w$ | $c_1$ | $c_2$, K |
|---|---|---|
| 0.01 | 7.44 | 262 |
| 0.007 | 4.95 | 170 |
| 0.005 | 6.96 | 226 |
| 0.003 | 10.9 | 389 |
| 0.002 | 10.8 | 386 |

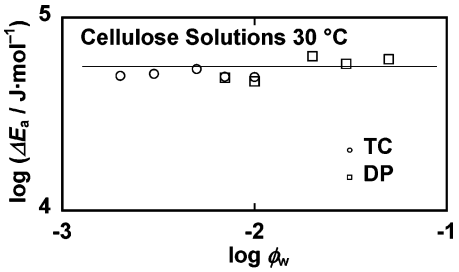


**Figure 8.** Dependence of activation energy, $\Delta E_a$, on weight fraction of polymer, $\phi_w$, for TC solution and DP solution in 8 wt % LiCl/DMI at 30 °C.

Also for the DP solutions at various concentrations, the values of $\Delta E_a$ were estimated in the same manner.

The $\phi_w$-dependence of $\Delta E_a$ is shown in a double logarithmic plot for the TC and DP solutions (Figure 8). The values of $\Delta E_a$ can be regarded as almost constant (ca. 53 kJ/mol) independent of the sort and concentration of the cellulose solutions. This means that the energy barrier of height $\Delta E_a$ that cellulose molecules in the solutions have to overcome in the viscoelastic relaxation process is independent of the concentration in the semidilute regime. In the case of cellulose solutions, one may expect that the increment of the cellulose concentration in the solution, especially in semidilute regime, will strongly promote some complicated polymer−polymer interactions such as intermolecular hydrogen bonds due to the presence of a large number of hydroxyl groups on a cellulose molecule. However, this result shows that such intermolecular interactions will make an insignificant contribution to the relaxation process and the flow properties. Accordingly, it is expected that physical entanglement (i.e., the topological constraint) is the major interpolymer interaction in the semidilute regime and that others may be negligible in terms of the effect on the flow properties. Despite too much simplification of the situation, this speculation is considered to be valid, considering the fact that similar behavior was observed for curdlan (1,3-$\beta$-D-glucan) in 0.1 N NaOH aqueous solution and in DMSO solution.[32]

**Concentration Dependence of Plateau Modulus.** Figures 4 and 5 show also the reproducibility of the master curves of $G'(\omega)$ and $G''(\omega)$ with appropriate combinations of $\tau_p$ and $G_p$ for the TC and the DP solutions in 8 wt % LiCl/DMI, respectively. These calculation curves of $G'(\omega)$ and $G''(\omega)$ are in good agreement with the experimental data except in the lower frequency regions of the TC solutions at $\phi_w = 0.007$ and 0.01. This disagreement shows the change in the apparent shape of the curves of the viscoelastic functions around the terminal zone with increasing concentration. In general, polymer solutions at different concentrations show similarity and universality in the shape of their viscoelastic curves.[33,34] This change is seldom observed within such a narrow concentration range as long as nothing special occurs such as gelation and formation of some association. It is unclear what the change means, but it may suggest some change of the properties regarding polymer dynamics, such as the relaxation process and mechanism with increasing concentration. Thus, it is expected that it largely affects properties on a long time scale, such as the longest relaxation time, the viscosity, and the steady-state compliance of the solution, but hardly affects short-time-scale properties including the plateau modulus, $G_N$.

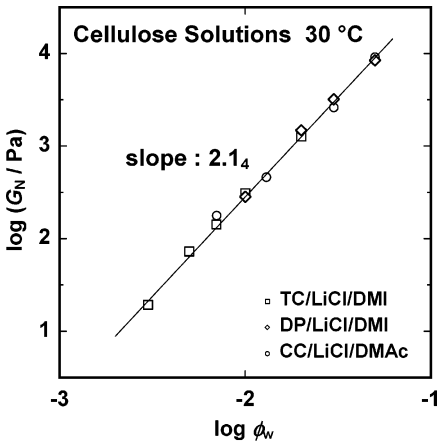


**Figure 9.** Dependence of plateau modulus, $G_N$, on weight fraction of polymer, $\phi_w$, for TC solution and DP solution in 8 wt % LiCl/DMI and CC solution in 8 wt % LiCl/DMAc at 30 °C.

The $\phi_w$-dependence of $G_N$ is shown in Figure 9 for the TC and DP solutions. The figure also shows that of the CC solution in 8 wt % LiCl/DMAc from the previous work.[17] Regardless of the kind of the cellulose samples and the solvents, the dependence can be represented by an identical straight line with a slope of $2.1_4$ in a double logarithmic plot, signifying that $G_N$ is in proportion to $\phi_w^{2.14}$. According to the scaling theory,[35] the exponent $\beta$ in the relation of $G_N \propto c^\beta$ is expected to be 2.25 for flexible polymer solutions. The theory of Doi−Edwards[36] predicts $\beta \approx 2.5$. Experimentally, for example, the relation of $G_N \propto c^{2.3}$ was observed for polystyrene and poly(α-methylstyrene) in chlorinated biphenyl solution.[33] The exponent of $2.1_4$ seems slightly smaller compared to these theoretical and experimental results, but it is probably valid with to regard the TC, the DP, and the CC molecules as flexible enough to form an entanglement network structure because the exponent is apt to fluctuate slightly depending on the solvent quality.

The relation between $G_N$ and $\phi_w$, including a numerical factor, can be expressed as the following equation:

$$G_N = (5.49 \times 10^6)\phi_w^{2.14}\ \text{Pa} \qquad (6)$$

The value of the front factor in eq 6 appears to correspond to that of the plateau modulus of pure cellulose in a molten state (i.e., cellulose melt), because $\phi_w = 1$ means that a system contains only polymer solute and no amount of solvent. No one can confirm that this value is actually equal to that of the cellulose melt because the cellulose melt is not available. However, it is probably overly hasty and inapposite to regard the front factor of 5.49 MPa as the value of the plateau modulus of the cellulose melt. From the

structural aspects, it is quite natural and reasonable to consider an actual polymer melt to be different from a *hypothetical melt*, which is created hypothetically from solution merely by increasing the number of the polymer chains in solution (i.e., extrapolation to $\phi_w = 1$). This will be clearly accepted considering the following possibility: the chain structure in the hypothetical melt reflects that in the primitive solution, and thus, the value of the front factor can change if the kind of solvent changes. Actually, the value of $G_N$ of the another hypothetical cellulose melt was estimated to be 2.21 MPa from cellulose/NMMO solution,[37] which is much smaller than our result. Thus, the front factor corresponds not to the unique value of the plateau modulus of the cellulose melt, but to that of one of the hypothetical cellulose melts from the cellulose solution in 8 wt % LiCl/DMAc and 8 wt % LiCl/DMI.

On the basis of this speculation, we can further develop the discussion on the chain structure of the TC, the DP, and the CC molecules in the solution. Fetters et al.[38] proposed that the plateau modulus and the chain dimension, $\langle R^2\rangle_0/M$, can be connected with each other for flexible polymer melts using a parameter, $p$, called packing length, by following equation:

$$G_N = ({}^4/_5)B^2kTp^{-3} \tag{7}$$

$$p = M/\langle R^2\rangle_0\rho N_A \tag{8}$$

where $k$, $T$, $\langle R^2\rangle_0$, and $\rho$ represent the Boltzmann constant, the absolute temperature, the unperturbed mean-square end-to-end distance (the subscript "0" denotes the unperturbed state), and polymer density, respectively. $B$ is a constant equal to $5.65 \times 10^{-2}$, which has been experimentally determined at 298 K and here can be regarded as independent of the temperature.[38] As is clear from eqs 7 and 8, the fact that for the TC, the DP, and the CC solutions the $\phi_w$-dependence of $G_N$ is represented by one identical straight line means that all of these cellulose molecules have an identical chain dimension. This result strongly supports the suggestion about the chain structure drawn from the dilute solution properties, which is discussed in the section "Size of the TC Molecule".

Provided that the value of $B$ is applicable to a hypothetical melt, eqs 7 and 8 give $\langle R^2\rangle_0/M = 8.87$ nm$^2$·mol·kg$^{-1}$ by substituting $G_N = 5.49 \times 10^6$ Pa, $T = 303$ K, and $\rho = 1.5 \times 10^3$ kg/m$^3$. Here, we used the value of the density of the actual cellulose crystal as that of the hypothetical cellulose melt. Using the relation of $\langle R^2\rangle_0 = 6\langle R_g^2\rangle_0$, we estimate the $\langle R_g^2\rangle_0$ values of the TC, the DP, and the CC molecules to be 78.1, 38.1, and 50.1 nm, respectively. It is very interesting that these values are very close to the corresponding $R_g$ values of the freely rotating chain model having a bond angle of 125° and a segment length of 0.564 nm: $R_{g,model} = 71.1$ nm (TC), $R_{g,model} = 34.7$ nm (DP), $R_{g,model} = 45.6$ nm (CC). In addition, it is more interesting that the $R_g$ values of the perturbed chain of the TC and the CC molecules are estimated to be 200 and 115 nm, respectively, on the assumption that the relation of $R_g = bN^v/\sqrt{6}$ will hold with an exponent $v$ of $0.61_7$, a bond length $b$ of 0.564 nm, and the number of segments $N$ of $2.55 \times 10^4$ (TC) and of $1.05 \times 10^4$ (CC). This suggests that the conformation of the TC and the CC molecules in the solution can be roughly regarded as almost equivalent to that of a Gaussian chain in a perturbed state.

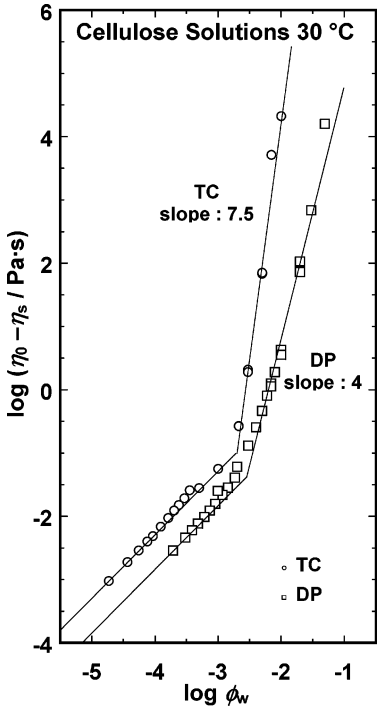


**Figure 10.** Dependence of $\eta_0 - \eta_s$ on $\phi_w$ for TC solution and DP solution in 8 wt % LiCl/DMI at 30 °C. For each solution, the dependence can be approximately represented by two straight lines with a slope of 1 in the dilute region and a slope of 7.5 (TC) or 4 (DP) in the semidilute region.

**Concentration Dependence of Zero Shear Viscosity.** For the TC and the DP solutions in 8 wt % LiCl/DMI, Figure 10 shows concentration ($\phi_w$) dependence of $\eta_0 - \eta_s$ in the form of double logarithmic plot. In this figure, the data from the measurements of the dynamic viscoelasticity, the limiting viscosity number, and the steady flow are simultaneously plotted. For both of the cellulose solutions, $\phi_w$-dependence of $\eta_0 - \eta_s$ can be represented approximately by two straight lines in the double logarithmic plot. The concentration at the point where the change of the slope of the straight line occurs is a kind of critical concentration, $\phi_{w,cr}$, at which the interpolymer interactions in the flow process change drastically.

A solution sufficiently below $\phi_{w,cr}$ can be roughly regarded as a dilute solution, where polymer molecules are dispersed separately. Strictly speaking, a dilute solution must be defined as a solution below the overlap concentration, $c^*$, as discussed above. In this concentration regime (i.e., dilute regime), many physical properties of the solution are expected from the dispersion state of the solute polymer to be proportional to the concentration. These cellulose solutions actually showed such proportional relation between $\eta_0 - \eta_s$ and $\phi_w$ in the dilute regime, as is clear from Figure 10. As the concentration increases above $\phi_{w,cr}$, the polymer chains are strongly overlapped and intermolecular interactions become predominant (i.e., semidilute region). According to these perspectives of the dispersion state of the solute polymer, various types of interactions can be reflected in

the $\phi_w$-dependence of $\eta_0 - \eta_s$ above $\phi_{w,cr}$. Actually, various values of the exponent $\alpha$ in $\eta_0 \propto c^{\alpha}$, ranging approximately from 4 to 6, have been experimentally obtained for many semidilute solutions of flexible polymers including biopolymers.[39−41] In many cases, thus, it is extremely difficult to estimate only the effect of the interaction purely by physical entanglement of polymer chains (i.e., universal nature for flexible polymers) from the actual concentration dependence of $\eta_0$. It probably involves various contributions of additional interactions. However, the discussion on the activation energy as described above can simplify the situation; that is, it can be hypothesized that only topological constraints have to be taken into account as an interpolymer interaction for these cellulose solutions in the flow process. This means that only the effect of the entanglements may be reflected in the $\phi_w$-dependence of $\eta_0 - \eta_s$. For the DP solution in 8 wt % LiCl/DMI, the relation of $\eta_0 - \eta_s \propto \phi_w^4$ was observed in semidilute regime as shown in Figure 10. This $\phi_w$-dependence is identical to that observed for the DP and the CC solutions in 8 wt % LiCl/DMAc, as already reported in the previous paper.[17] The same speculation can apply to the results of the DP solution in 8 wt % LiCl/DMI; that is, also in 8 wt % LiCl/DMI the DP molecules take a similar conformation to that in 8 wt % LiCl/DMAc. This conclusion supports the expectation that the difference in the $[\eta]$ values of the DP in these two solvents is insignificant. This means that the conformations of the DP molecules in those two solvents are almost equal in terms of rheological properties of the solutions.

The TC solutions exhibited the relation of $\eta_0 - \eta_s \propto \phi_w^{7.5}$. The fact is known that the exponent $\alpha$ becomes larger as the quality of the solvent descends,[39] but as far as we know, no theory can tell what the exponent of 7.5 indicates. According to the above speculation, the dependence indicates at least that the flow behavior of the TC solution is far from that of a flexible polymer solution. This conclusion appears to be inconsistent with that from the dilute solution properties and the concentration dependence of the plateau modulus of the solutions; that is, the conclusion that all these celluloses have the same structure of a flexible chain. At the present time, we cannot explain explicitly this inconsistency but can add some remarks about what is responsible for the discrepancy. As a clue to the elucidation, first of all, we should point out that zero shear rate viscosity of a polymer solution is one of the physical properties that are closely related to dynamics of polymers, whereas plateau modulus and radius of gyration are static physical quantities. What such difference means is well understood in comparison with a typical semidilute solution of a flexible polymer and a polymeric gel of a cross-linked solution. For both systems, the theoretical relation of $G_N \propto c^{2.25}$ will hold, because the relation reflects the static structure of the system. On the other hand, the viscosities of these systems are utterly different; that is, solutions have finite viscosities but gels infinite ones. From this viewpoint, that discrepant result is explainable: the TC solutions have a similar chain structure to those of the DP and the CC solutions but the relaxation process and mechanism of the molecular chains of the TC in the solution are different from those of the DP and the CC. This difference in dynamical features is probably related to the change in the shape of the curves $G'(\omega)$ and $G''(\omega)$ with increasing concentration.

**Normalized Plot for Concentration Dependence of Solution Viscosity.** To draw normalized plots of the concentration dependence of the solution viscosity, we chose the Bueche parameter, $\phi_w M_w$, and the overlap parameter, $\phi_w[\eta]\rho_{solv}$, as reduced concentration, and the specific viscosity, $\eta_{sp}$, as reduced viscosity. Here, $\rho_{solv}$ denotes density of the solvent. These two kinds of reduced concentrations include some molecular characteristics from different measurements for dilute solutions. Thus, creating the normalized plots with these kinds of normalized parameters enables us not only to find out essential features and properties of the systems but also to confirm the accuracy of the results from all of the underlying measurements. With the Bueche parameter, the concentration dependence of $\eta_{sp}$ is shown in Figure 11a for the TC and the DP solutions in 8 wt % LiCl/DMI. In terms of the number of intermolecular interaction points per unit volume, it is expected that the difference in molecular weight can be reduced or compensated by plotting the solution viscosity against $\phi_w M_w$.[16,42−44] As shown in Figure 11a, actually, the relationship between log $\phi_w M_w$ and log $\eta_{sp}$ can be superimposed fairly well in the dilute region for both cellulose solutions. This good superposition in the dilute region shows that each cellulose sample has similar molecular properties in dilute solution except for the molecular weight and related characteristics. Moreover, it also indicates, as is mentioned above, that the determination of the $M_w$ for each cellulose sample was properly performed. This result gives suggestive information about the similarities and differences between these cellulose samples: the TC molecules are similar to the DP molecules in respect of characteristics of individual molecular chains but different in properties of many chain systems.

Figure 11b shows the double logarithmic plot of $\eta_{sp}$ versus the overlap parameter, $\phi_w[\eta]\rho_{solv}$, for the TC and DP solutions in 8 wt % LiCl/DMI and also for the CC, the DP, and the BC solutions in 8 wt % LiCl/DMAc.[17] Strictly speaking, the density of the solution, $\rho_{soln}$, must be used for the overlap parameter instead of $\rho_{solv}$. If the concentration of the solution is not so high, $\rho_{soln}$ can be regarded as almost equal to $\rho_{solv}$, and thus the difference between $\phi_w[\eta]\rho_{solv}$ and $\phi_w[\eta]\rho_{soln}$ is negligible. In general, the overlap parameter is more suitable as a reduced concentration for showing the concentration dependence of solution viscosity than the Bueche parameter, since the limiting viscosity number is a measure of hydrodynamic volume of the solute polymer molecule in solution.[41,42,45] Actually, by use of this parameter all of the data are superimposed excellently in the dilute region, where the intermolecular interactions can be neglected. This very good agreement demonstrates the suitability of the parameter as well as the accuracy of the measurements of $[\eta]$. For the DP and the CC solutions, the data can also be superimposed well in the semidilute region, where the intermolecular interactions become predominant, regardless of the kind of the solvent. This suggests that cellulose molecules of the CC and the DP, which are derived from plant sources, are different only in hydrodynamic volume of polymer but

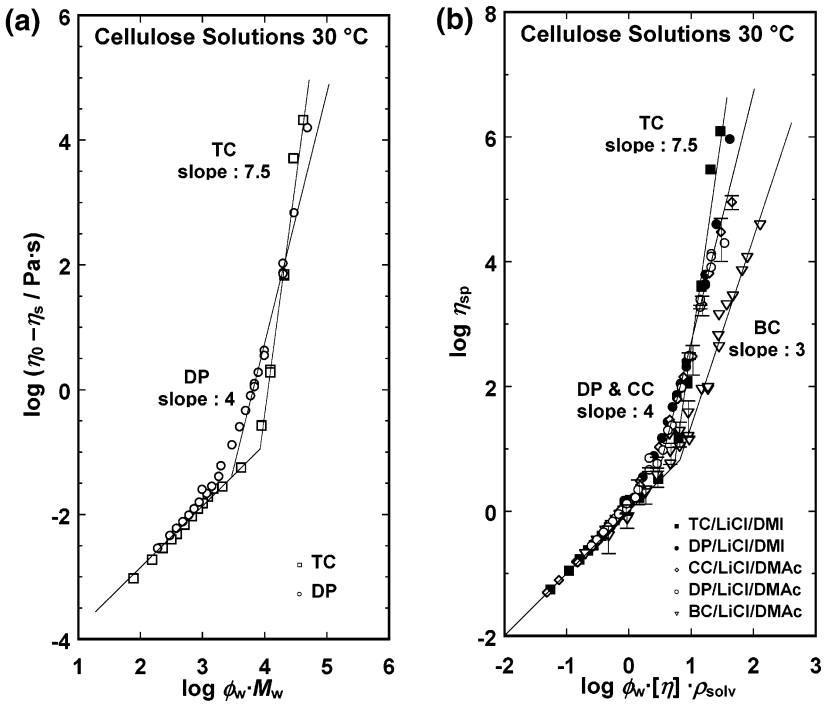


**Figure 11.** Dependence of (a) $\eta_{sp}$ on $\phi_w M_w$ for TC and DP solutions in 8 wt % LiCl/DMI at 30 °C and (b) $\eta_{sp}$ on $\phi_w[\eta]\rho_{solv}$ for TC and DP solutions in 8 wt % LiCl/DMI and also for CC, BC, and DP solutions in 8 wt % LiCl/DMAc at 30 °C. A parameter of $\phi_w[\eta]\rho_{solv}$ can be regarded as almost equal to the overlapping parameter, $c[\eta]$, which is a kind of reduced concentration.

otherwise identical in terms of the flow behavior or hydrodynamic properties. On the other hand, the BC solution in 8 wt % LiCl/DMAc and the TC solution in 8 wt % LiCl/DMI showed different dependence from these solutions of plant celluloses in the semidilute regions. This difference reflects the difference in dynamical properties of the flow behavior, which fails to be essentially compensated for by the normalization using the overlap parameter. As for the BC solution, we have reported in the previous paper that the difference in the flow behavior comes from the difference in a molecular conformation in the solution.[17] For the TC solution, it is not clear what difference of the dynamical properties is reflected in the relation of $\eta_{sp} \propto \phi_w^{7.5}$. A recent excellent research by Saalwächter and Burchard[15] has revealed some deviations from the predictions by Doi−Edwards theory using the reptation model as to dynamic molecular properties (e.g., reptation time, $\tau_d$) of cellulose with high molecular weight ($M_w = 2.22 \times 10^6$; $R_g = 145$ nm) in Cd-tren solution. These results suggest that dynamic molecular properties of cellulose must be of greater importance for the comprehensive systematization of structure and physical properties of cellulose from various biological origins. Future investigation will explicate its molecular dynamics, as well as its detailed and precise static structure, on the basis of accepted molecular theories.

## Conclusion

The SLS and viscometric measurements revealed the molecular characteristics of the TC molecules in 8 wt % LiCl/DMI solution: $M_w = 4.13 \times 10^6$; $[\eta] = 2645$ mL/g. These values are much greater than those of other cellulose samples such as the DP, the CC, and the BC. The $R_g$ value of the TC was expected to be 184−188 nm, suggesting that the TC molecules have similar structure to the CC in 8 wt % LiCl/DMAc solution with $\upsilon = 0.61_7$.

The dynamic viscoelasticity measurements gave us much suggestive information on both dynamic properties and static structure of the solution. Qualitatively, the TC solutions, as well as the DP solutions, showed typical viscoelastic behavior of isotropic flexible polymer solutions. Due to the size of the TC molecule, however, the obvious appearance of plateau region was observed in the viscoelastic curves of $\omega$-dependence of dynamic moduli at very low concentration, and the change in the shape of the curves with increasing concentration was uncommonly remarkable within the extremely narrow concentration range. The concentration dependence of the plateau modulus, $G_N \propto \phi_w^{2.14}$, indicated the formation of the network structure in the solution by chain entanglements. This dependence was identical with those for the DP solution in 8 wt % LiCl/DMI and the CC solution in 8 wt % LiCl/DMAc, indicating that the TC, the DP, and the CC have the same chain structure (Gaussian chain conformation in a perturbed state). Regarding the molecular structure, this result and the results from the SLS measurements strongly supported each other. Zero shear viscosity of the TC solution was in proportion to $\phi_w^{7.5}$. This concentration dependence is much more striking than those for the other cellulose solutions. The theory of Doi−Edwards predicts the exponent of ca. 4 for a flexible polymer and of 3 for a rodlike polymer. However, no theory can explain the exponent of 7.5. This difference may show the difference in dynamical properties in the relaxation process.

**Acknowledgment.** The authors express their gratitude to Professor F. Horii, Kyoto University, for his kind provision of the tunicate cellulose sample. This work was supported

by a Grant-in-Aid for Scientific Research (No. 12460076) from the Ministry of Education, Science, Sports and Culture of Japan.

## References and Notes

(1) De Leo, G.; Patricolo, E.; D'Ancona Lunetta, G. *Acta Zool. (Stockholm)* **1977**, *58*, 135−141.
(2) D'Ancona Lunetta, G. *Acta Embryol. Morphol. Exp.* **1983**, *4*, 137−149.
(3) Nobles, D. R.; Romanovicz, D. K.; Brown, R. M., Jr. *Plant Physiol.* **2001**, *127*, 529−542.
(4) Read, S. M.; Bacic, T. *Science* **2002**, *295*, 59−60.
(5) Roberts, A. W.; Roberts, E. M.; Delmer, D. P. *Mesotaenium caldariorum*. *Eukaryotic Cell* **2002**, *1*, 847−855.
(6) Atalla, R. H.; VanderHart, D. L. *Science* **1984**, *223*, 283−285.
(7) VanderHart, D. L.; Atalla, R. H. *Macromolecules* **1984**, *17*, 1465−1472.
(8) Horii, F. In *Wood and Cellulosic Chemistry*, 2nd ed.; Hon, D. N.-S., Shiraishi, N., Eds.; Marcel Dekker, Inc.: New York, 2001; Chapter 3.
(9) Atalla, R. H. *Preprints of 1st International Cellulose Conference in Kyoto*, Kyoto, 2002; Presentation O2-08; Press-net: Kyoto, Japan; pp 21.
(10) McCormick, C. L. U. S. Patent 4,278,790, 1981.
(11) Turbak, A.; El-Kafrawy, A.; Snyder, F. W.; Auerbach, A. B. U. S. Patent 4,302,252, 1981.
(12) McCormick, C. L.; Lichtowich, D. K. *J. Polym. Sci.: Polym. Lett. Ed.* **1979**, *17*, 479−484.
(13) McCormick, C. L.; Callais, P. A.; Hutchinson, B. H., Jr. *Macromolecules* **1985**, *18*, 2394−2401.
(14) Saalwächter, K.; Burchard, W.; Klüfers, P.; Kettenbach, G.; Mayer, P.; Klemm, D.; Dugarmaa, S. *Macromolecules* **2000**, *33*, 4094−4107.
(15) Saalwächter, K.; Burchard, W. *Macromolecules* **2001**, *34*, 5587−5598.
(16) Matsumoto, T.; Tatsumi, D.; Tamai, N.; Takaki, T. *Cellulose* **2001**, *8*, 275−282.
(17) Tamai, N.; Aono, H.; Tatsumi, D.; Matsumoto, T. *J. Soc. Rheol., Jpn.* **2003**, *31*, 119−130.
(18) El-Kafrawy, A. *J. Polym. Sci.* **1982**, *27*, 2435−2443.
(19) Namikoshi, H. Japan Kokai Patent 59 124933, 1984.
(20) Edgar, J.; Bogan, T. European Patent WO 96 20960, 1996.
(21) This d*n*/d*c* value of 0.0406 mL/g was determined using another natural polysaccharide of curdlan (1,3-*β*-D-glucan), which consists of anhydroglucopyranose only. The TC solutions showed large fluctuation of the refractive index during the measurements. It is, thus, quite difficult to get a reliable value of d*n*/d*c* for the TC solution by direct measurements. McCormick et al. has reported the difficulties of the determination of the d*n*/d*c* values for the cellulose solutions in 9 wt % LiCl/DMAc.[13] They showed some variance of the values among nine samples of the solutions by repeated determinations. Saalwächter et al. has proposed that the difference of the d*n*/d*c* value between amylose and cellulose solutions in water containing metal complexes is negligible because both polysaccharides are composed of the same monomer units of anhydroglucopyranose rings.[14] Considering all of these things, we used the d*n*/d*c* value of 0.0406 mL/g as that for the TC solution. Needless to say, we confirm the reliability of this d*n*/d*c* value of 0.0406 mL/g by evaluating the $M_w$ value of curdlan in this solvent ($M_w = 7.1 \times 10^5$). This is almost equal to the value of $7.4 \times 10^5$, which was determined at 60 °C using 0.1 N NaOH aqueous solution.
(22) Ferry, J. D. *Viscoelastic Properties of Polymers*, 2nd ed.; John Wiley & Sons: New York, 1970; Chapter 11.
(23) Billmeyer, F. W., Jr. *Textbook of Polymer Science*; John Wiley & Sons: New York and London, 1962; pp 79−82.
(24) Rouse, P. E. *J. Chem. Phys.* **1953**, *21*, 1272−1280.
(25) Osaki, K.; Inoue, T.; Uematsu, T. *J. Polym. Sci., Part B: Polym. Phys.* **2001**, *39*, 211−217.
(26) Cox, W. P.; Merz, E. H. *J. Polym. Sci.* **1958**, *28*, 591.
(27) Schoff, C. K. In *Polymer Handbook*, 4th ed.; Brandrup, J., Immergut, E. H., Grulke, E. A., Eds.; John Wiley & Sons: New York, 1999; pp VII, 265−267.
(28) Doi, M.; Edwards, S. F. *The Theory of Polymer Dynamics*; Oxford University Press: New York, 1986; Chapter 4, p 114.
(29) Doi, M.; Edwards, S. F. *The Theory of Polymer Dynamics*; Oxford University Press: New York, 1986; Chapter 5, p 141.
(30) Nakamura, Y.; Norisuye, T.; Teramoto, A. *J. Polym. Sci., Part B: Polym. Phys.* **1991**, *29*, 153−159.
(31) Daňhelka, J.; Netopilík, M.; Bohdaneck×c6, M. *J. Polym. Sci., Part B: Polym. Phys.* **1987**, *25*, 1801−1815.
(32) Tada, T.; Tamai, N.; Matsumoto, T.; Masuda, T. *Biopolymers* **2001**, *58*, 129−137.
(33) Osaki, K.; Takatori, E.; Tsunashima, Y.; Kurata, M. *Macromolecules* **1987**, *20*, 525−529.
(34) Carella, J. M.; Graessley, W. W.; Fetters, L. J. *Macromolecules* **1984**, *17*, 2775−2786.
(35) de Gennes, P.-G. *Scaling Concepts in Polymer Physics*; Cornell University Press: Ithaca, NY, 1979.
(36) Doi, M.; Edwards, S. F. *J. Chem. Soc., Faraday Trans. 2* **1978**, *74*, 1818−1832.
(37) Blachot, J.-F.; Brunet, N.; Navard, P.; Cavaillé, J.-Y. *Rheol. Acta* **1998**, *37*, 107−114.
(38) Fetters, L. J.; Lohse, D. J.; Richter, D.; Witten, T. A.; Zirkel, A. *Macromolecules* **1994**, *27*, 4639−4647.
(39) Grigorescu, G.; Kulicke, W.-M. *Adv. Polym. Sci.* **2000**, *152*, 1−40.
(40) Launay, B.; Cuvelier, G.; Martinez-Reyes, S. *Carbohydr. Polym.* **1997**, *34*, 385.
(41) Onogi, S.; Masuda, T.; Miyanaga, N.; Kimura, Y. *J. Polym. Sci., Part A-2* **1967**, *5*, 899−913.
(42) Graessley, W. W. *Adv. Polym. Sci.* **1974**, *16*, 38−72.
(43) Berry, G. C.; Nakayasu, H.; Fox, T. G. *J. Polym. Sci.: Phys. Ed.* **1979**, *17*, 1825−1844.
(44) Matsumoto, T.; Kawai, M.; Masuda, T. *Biorheology* **1992**, *29*, 411−417.
(45) Morris, E. R.; Cutler, A. N.; Ross-Murphy, S. B.; Rees, D. A.; Price, J. *Carbohydr. Polym.* **1981**, *1*, 5−21.

BM034236H